Int. j. adv. multidisc. res. stud. 2026; 6(5):516-520

Received: 26-07-2026
Accepted: 06-09-2026

International Journal of Advanced Multidisciplinary Research and Studies

ISSN: 2583-049X

MHD Maxwell Fluid Flow Over a Vertical Cone with Thermal Radiation and Cattaneo-Christov Heat Flux: A Numerical Investigation

[1] **Sagili Navaneeswara Reddy,** [2] **Sane SreeLakshmi**
[1] Department of Mathematics, Government College for Men (A), Kadapa, Andhra Pradesh, India
[2] Department of Mathematics, NSPR Government Degree College for Women, Hindupur, Andhra Pradesh - 515201, India

DOI: https://doi.org/10.62225/2583049X.2026.6.5.6879
Corresponding Author: **Sagili Navaneeswara Reddy**

Abstract
This study presents a numerical investigation of magnetohydrodynamic (MHD) flow of a Maxwell non-Newtonian fluid over a vertical cone, incorporating thermal radiation and Cattaneo-Christov heat flux effects. The governing partial differential equations are transformed into a system of ordinary differential equations using appropriate similarity transformations and solved numerically using the bvp4c solver in MATLAB. The influence of key dimensionless parameters, including the magnetic field parameter (Hartmann number), Weissenberg number, thermal radiation parameter, and thermal relaxation parameter, on velocity and temperature profiles is systematically analysed. Results indicate that increasing the magnetic field parameter intensifies the Lorentz force, which acts as a resistive drag that significantly reduces fluid velocity. Similarly, higher Weissenberg numbers enhance fluid elasticity, increasing resistance to deformation and suppressing momentum diffusion, thereby lowering velocity profiles. Conversely, thermal radiation enhances heat absorption within the fluid, acting as a volumetric heat source that elevates temperature profiles, while the thermal relaxation parameter reduces effective thermal diffusivity, resulting in decreased temperatures. Additionally, multiple linear regression analysis is employed to develop predictive models for skin friction coefficient and Nusselt number as functions of the governing parameters. The regression models demonstrate that the skin friction coefficient increases with both magnetic parameter and Weissenberg number, while the Nusselt number exhibits positive correlations with thermal radiation and thermal relaxation parameters.

Keywords: Weissenberg Number, bvp4c, Magnetic Field, Prandtl Number, Non-Fourier Heat Flux

1. Introduction

The study of non-Newtonian fluid flow over a cone holds considerable significance due to its extensive applications across various engineering and industrial domains. The conical geometry is pivotal in processes like polymer spin coating, where precise thermal and flow control is vital for producing electro-conductive polymers. Furthermore, such flows are integral to the design of conical diffusers, medical devices, and rheometric equipment applications. This research also aids in optimizing heat exchanger design, enhancing energy transfer in thermal equipment, and improving the efficiency of gas turbine engines. The ability to model and control these flows through factors like magnetic fields and permeability is crucial for advancements in micro-cooling systems, micromixers, and chemical reactor technology. Sajjad-ur-Rehman *et al.* [1] conducted a numerical investigation on three-dimensional Casson fluid flow over an exponentially stretching heated surface. They employed the Runge–Kutta–Felberg method alongside homotopy analysis and its optimal variant to validate the solutions for momentum and energy equations under similarity transformations. Non-Newtonian Casson fluids exhibited higher wall friction coefficients than Newtonian fluids, whereas the heat transfer rate (Nusselt number) was more pronounced in the Newtonian case across varying temperature exponents. Additionally, the velocity profiles declined with increasing Casson parameter and stretching ratio along the streamwise direction, while the temperature profile rose with higher values of both the Casson parameter and the temperature exponent. Rashidi *et al.* [2] analytically investigated the convective magnetohydrodynamic flow of a third-grade non-Newtonian fluid over a linearly stretching sheet, incorporating entropy generation analysis. They employed the optimal homotopy analysis method to solve the transformed ordinary differential equations and examined the effects of magnetic field, Biot number, and Prandtl number on velocity and temperature fields. The thermal boundary layer thickness diminished with rising Prandtl number, while the magnetic parameter enhanced both temperature distribution and entropy generation near the sheet. Furthermore, entropy generation intensified with increasing Reynolds, Brinkman, Hartmann, and Biot numbers, whereas the third-grade fluid parameter exhibited a non-monotonic influence on entropy production along the boundary layer. Amanulla *et al.* [3] numerically examined the steady two-dimensional free convective MHD flow of a Carreau non-Newtonian fluid over an isothermal sphere, incorporating velocity slip and temperature jump conditions at the surface. Khan *et al.* [4] numerically investigated the steady two-dimensional flow of a Carreau non-Newtonian fluid over an inclined shrinking surface, incorporating the effects of infinite shear rate viscosity. Maleki *et al.* [5] numerically investigated the boundary layer flow and heat transfer of pseudo-plastic non-Newtonian nanofluids over a permeable flat plate, considering Cu, CuO, TiO_2 and Al_2O_3 nanoparticles dispersed in CMC/water base fluid. Mozafarie and Javaherdeh [6] numerically investigated the flow and heat transfer characteristics of a non-Newtonian power-law fluid (soursop juice) flowing through the annulus of a double-pipe heat exchanger equipped with helical fins around the inner tube. Kempannagari *et al.* [7] numerically examined the magnetohydrodynamic stagnation-point flow of a micropolar non-Newtonian fluid over an exponentially stretching curved surface, incorporating Joule heating, nonlinear thermal radiation, variable thermal conductivity, and non-uniform heat source/sink effects. Selvi *et al.* [8] analytically studied the creeping flow around a Reiner–Rivlin non-Newtonian liquid droplet surrounded by a Newtonian liquid shell and embedded in a porous medium, using the Brinkman, Stokes, and Reiner–Rivlin equations for the respective regions. Ali *et al.* [9] numerically investigated the g-jitter-induced mixed convection flow of a micropolar non-Newtonian fluid over an inclined stretching sheet under the influence of a magnetic field and heat source/sink. Khashi'ie *et al.* [10] numerically investigated the magnetohydrodynamic radiative heat transfer of a Reiner–Philippoff non-Newtonian fluid over a nonlinearly shrinking sheet, incorporating viscous dissipation and Joule heating effects. Vishalakshi *et al.* [11] analytically investigated the three-dimensional magnetohydrodynamic flow of a Walters' liquid B non-Newtonian fluid over a porous stretching/shrinking sheet under an inclined magnetic field, incorporating thermal radiation and mass transpiration effects. Mahabaleshwar *et al.* [12] analytically examined the axisymmetric magnetohydrodynamic flow of a Casson non-Newtonian fluid over a nonlinear permeable stretching/shrinking surface, incorporating thermal radiation and Navier slip effects. Al Qahtani *et al.* [13] numerically investigated the non-similar flow of a generalized Newtonian (Cross) liquid over a vertical porous surface under the influence of nonlinear radiation, Newtonian heating, magnetic field, and gravitational effects. They employed a three-level truncation non-similarity approach to convert the partial differential equations into ordinary differential equations and solved them using a collocation method in MATLAB. Later, various authors [14-19] discussed different non-Newtonian fluid movements across distinct frameworks.

While extensive research has been dedicated to non-Newtonian fluid flows across various geometries, the combined influence of magnetohydrodynamic effects, thermal radiation, and the non-Fourier Cattaneo-Christov heat flux model on Maxwell fluid over a vertical conical surface remains underexplored. Existing studies have largely focused on stretching sheets or flat plates, with limited attention to conical configurations that are practically relevant in polymer processing and thermal equipment. Furthermore, the majority of prior investigations have relied on classical Fourier's law, neglecting the thermal relaxation time that characterizes heat propagation in viscoelastic fluids. This research addresses these gaps by developing a comprehensive numerical framework that simultaneously accounts for magnetic field interactions, radiative heat transfer, and the Cattaneo-Christov formulation for Maxwell fluid flow over a vertical cone. The significance of this work lies in its potential to enhance the predictive capability for thermal and flow behavior in conical geometries, thereby contributing to improved design and efficiency in industrial applications such as heat exchangers, spin coating processes, and rheological instrumentation. The findings from this investigation offer new insights into the coupled transport phenomena and provide a robust foundation for optimizing operational parameters in engineering systems involving complex fluid dynamics.

2. Mathematica Formulation

In this study, MHD flow of the Maxwell fluid over a vertical cone in the presence of thermal radiation and Cattaneo-Christov heat flux is considered. Flow is assumed to be laminar and steady. The cone has a radius $r = xSin\alpha$ and is pointing downward at a half-angle α. A uniform magnetic field B is applied perpendicular to the flow as shown in Fig 1.

Based on the assumptions made before, this investigation requires the following conditions and equations:

$$\frac{\partial(rv)}{\partial y}+\frac{\partial(ru)}{\partial x}=0 \tag{1}$$

$$u\frac{\partial u}{\partial x}+v\frac{\partial u}{\partial y}=\frac{\mu}{\rho}\frac{\partial^2 u}{\partial y^2}-\lambda\left(\frac{\partial^2 u}{\partial x^2}u^2+2uv\frac{\partial^2 u}{\partial x\partial y}+\frac{\partial^2 u}{\partial y^2}v^2\right)+g\beta_T(T-T_\infty)\mathrm{Cos}\,\alpha-\frac{\sigma B^2}{\rho}u \tag{2}$$

$$u\frac{\partial T}{\partial x}+v\frac{\partial T}{\partial y}=\left(\frac{k}{(\rho C_p)}+\frac{1}{(\rho C_p)}\frac{16\sigma^* T_\infty^3}{3k^*}\right)\frac{\partial^2 T}{\partial y^2}$$
$$-\delta\left(u^2\frac{\partial^2 T}{\partial x^2}+2uv\frac{\partial^2 T}{\partial x\partial y}+v^2\frac{\partial^2 T}{\partial y^2}+\frac{\partial T}{\partial x}\left(u\frac{\partial u}{\partial x}+v\frac{\partial v}{\partial y}\right)+\frac{\partial T}{\partial y}\left(u\frac{\partial v}{\partial x}+v\frac{\partial v}{\partial y}\right)\right) \tag{3}$$

$$\left.\begin{array}{l}\text{at } y=0: u=0, v=0, T=T_w,\\ \text{as } y\to\infty: T\to T_\infty, u\to 0.\end{array}\right\} \tag{4}$$

The following similarity transformations are employed to transform the governing equations:

$$\left.\begin{aligned} & u=\frac{\upsilon}{x}Gr^{1/2}f', v=-\frac{\upsilon}{4x}Gr^{1/4}\left(7f-\eta f'\right), Gr=\frac{g\beta_T \cos\alpha\left(T_w-T_\infty\right)x^3}{\upsilon^2}, \\ & \eta=\frac{y}{x}\left(Gr\right)^{0.25}, \theta\left(\eta\right)=\frac{T-T_\infty}{T_w-T_\infty}. \end{aligned}\right\} \qquad (5)$$

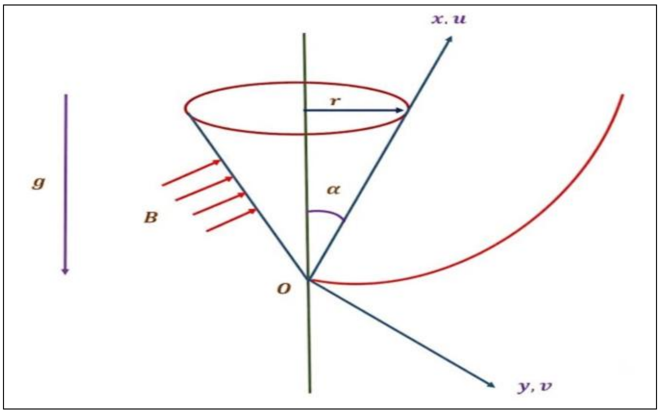

Fig 1: Flow diagram

Equation (1) can be readily satisfied by the terms presented in (5). The successful modification of equations (2-3) and conditions in (4) through integration of (5) yields the following result:

$$f'''+\frac{7}{4}ff''-\frac{1}{2}f'^2-We\left(\frac{49}{16}f^2f'''-\frac{1}{4}f'^3+\frac{3}{16}\eta f'^2f''-\frac{7}{8}ff'f''\right)+\theta-Mf'=0 \qquad (6)$$

$$\left(1+R\right)\frac{1}{\Pr}\theta''-\Gamma\left(\frac{63}{16}ff'\theta'+\frac{49}{16}f^2\theta''-\frac{3}{8}\eta ff''\theta'\right)+\frac{7}{4}f\theta'=0 \qquad (7)$$

$$\left.\begin{aligned} & \text{at } \eta=0: f=0, f'=0, \theta=1, \\ & \text{as } \eta\to\infty: f'\to 0, \theta\to 0. \end{aligned}\right\} \qquad (8)$$

Where

$$We=\frac{\upsilon Gr^{1/2}}{x^2}, M=\frac{\sigma B_0^2}{\rho\upsilon Gr^{0.5}}, B=\frac{B_0}{x}, \Gamma=\frac{\delta\upsilon}{x^2}Gr^{1/2}, R=\frac{16}{3}\frac{\sigma^* T_\infty^3}{kk^*}.$$

Skin friction coefficient and Nusselt number are defined as below:

$$\left(Gr\right)^{0.25}Cf=2f''\left(0\right), \left(Gr\right)^{-0.25}Nu=-\left(1+R\right)\theta'\left(0\right)$$

3. Results and Discussion

Equations (6 - 7) with the conditions (8) are solved using the bvp4c solver in MATLAB. The rise in the magnetic field parameter (Hartmann number) intensifies the Lorentz force, which acts as a resistive drag opposing the fluid motion. This retarding force significantly reduces the bulk flow velocity, a trend clearly illustrated by the decreasing velocity profiles in Fig 2. Fig 3 shows that as the Weissenberg number increases, the fluid's elastic relaxation time grows, which heightens its resistance to deformation and suppresses momentum diffusion. This enhanced elastic stress effectively thickens the fluid, thereby reducing the velocity gradient and causing a lower overall velocity profile. The rise in the thermal radiation parameter increases the temperature profile because it enhances the absorption of radiative heat within the fluid, adding more internal energy to the system. This additional radiative flux effectively acts as a volumetric heat source, which intensifies the thermal boundary layer and raises the local temperatures, as clearly demonstrated by the upward shift in the curves for increasing radiation values in Fig 4. Fig 4 shows that an increase in the thermal relaxation parameter (indicating a larger time lag between the heat flux and temperature gradient) reduces the effective thermal diffusivity of the medium. This slower heat propagation delays the inward movement of thermal energy, causing the temperature to drop significantly compared to the classical Fourier case.

3.1 Multiple Linear Regression

Multiple linear regression (MLR) is a powerful statistical tool used to model the linear relationship between a single dependent (response) variable and two or more independent (predictor) variables. Its primary importance lies in quantifying how each predictor influences the response, while controlling for the effects of others, thus enabling accurate predictions and identifying the most significant governing parameters in complex physical systems.

For the present problem, the skin friction coefficient (Cf) and Nusselt number (Nu) can be expressed as functions of key dimensionless parameters (e.g., magnetic field parameter and thermal radiation parameter). Before substituting the computed numerical values, the general regression models take the form:

$$Cf = \beta_0 + \beta_1 M + \beta_2 We \qquad (9)$$

$$Nu = \gamma_0 + \gamma_1 R + \gamma_2 \Gamma \qquad (10)$$

Where β_i and γ_i are the regression coefficients to be determined.

Now, substituting the actual numerical values from the 25-point dataset into these equations and performing the least-squares fitting yields the specific regression coefficients.

After substitution, equations (9 – 10) becomes:

$$Cf = 2.17 + 0.022 \cdot M + 0.1151 \cdot We \qquad (11)$$

$$Nu = 0.973 + 0.2738\,R + 0.2625\,\Gamma \qquad (12)$$

From equation (11), it is observed that the skin friction coefficient increases with a rise in both the magnetic parameter (M) and the Weissenberg number (We). The magnetic field generates a drag-like force called the Lorentz force, which resists the fluid motion and adds extra friction at the surface. Although the effect of M is relatively small, it still contributes positively to the skin friction. On the other hand, the Weissenberg number has a much stronger influence because it represents the elastic behaviour of the fluid. Higher elasticity means the fluid resists stretching and deformation more strongly, which increases the shear stress acting on the boundary wall. Thus, both parameters hinder the flow near the surface, leading to a higher skin friction coefficient. From equation (12), it is observed that the Nusselt number increases with a rise in both the radiation parameter (R) and the thermal relaxation parameter (Γ). The radiation parameter enhances heat transfer because thermal radiation provides an additional mode of energy transport apart from conduction and convection. As R increases, more heat energy is carried through radiation, which improves the overall rate of heat transfer at the surface. Similarly, the thermal relaxation parameter also shows a positive effect, meaning that within this regression model, an increase in Γ leads to better heat transfer. This suggests that under the specific conditions of the dataset, the delay in heat flow may actually allow more time for thermal energy to accumulate and be transferred effectively.

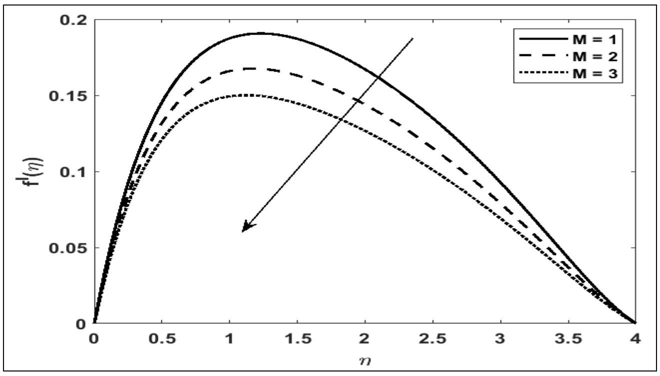

Fig 2: Impact of Magnetic field parameter on the velocity profile

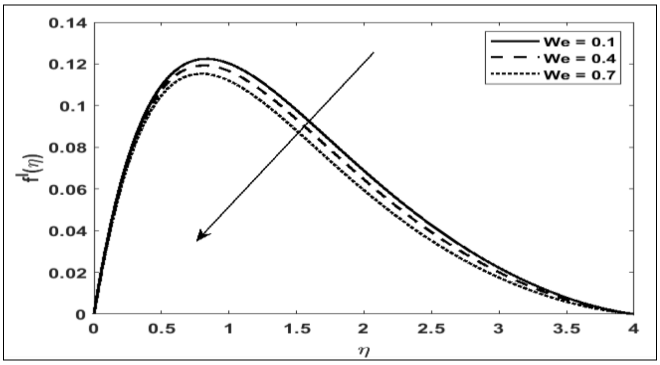

Fig 3: Impact of Weissenberg number on the velocity profile

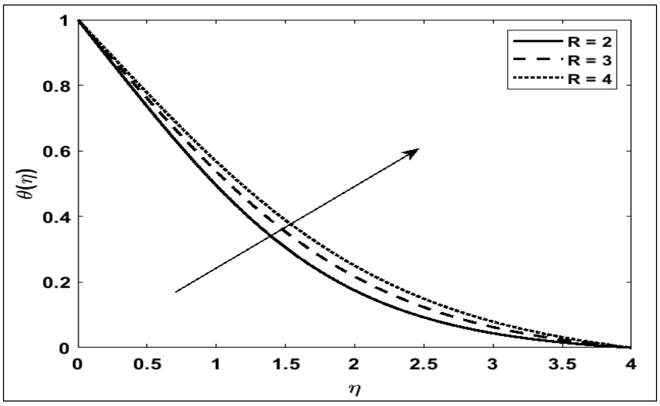

Fig 4: Impact of thermal radiation parameter on the temperature profile

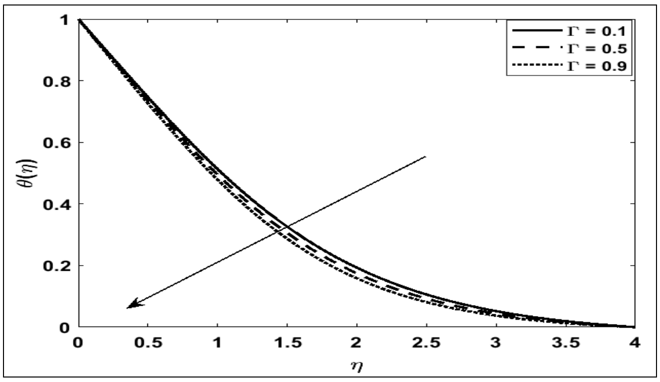

Fig 5: Impact of thermal relaxation parameter on the temperature profile

4. Conclusions

The present study numerically investigated the magnetohydrodynamic boundary layer flow of a Maxwell non-Newtonian fluid over a vertical cone, incorporating the effects of thermal radiation and Cattaneo-Christov heat flux. The governing partial differential equations were transformed into ordinary differential equations using similarity transformations and subsequently solved using the bvp4c solver in MATLAB. The influence of key physical parameters on velocity and temperature fields was systematically examined, and multiple linear regression models were developed to predict the skin friction coefficient and Nusselt number. The major findings of this investigation are summarized as follows:

- Rise in the magnetic field parameter causes a reduction in the velocity of the fluid.
- Fluid velocity decreases with the increase in the Weissenberg number.
- It is observed that there is a rise in the temperature of the fluid with the rise in the thermal radiation but the same decreases with the surge in the thermal relaxation parameter.
- It is noticed that there is a rise in the skin friction coefficient with the rise in both the magnetic field parameter and Weissenberg number.
- It is observed that the Nusselt number increases with a rise in both the radiation parameter and thermal relaxation parameter.

5. References

1. Sajjad-ur-Rehman Lee C, Nadeem S. Numerical study of non-Newtonian fluid flow over an exponentially stretching surface: An optimal HAM validation. Journal of the Brazilian Society of Mechanical Sciences and Engineering. 2017; 39(5):1589-1596.
2. Rashidi MM, Bagheri S, Momoniat E, Freidoonimehr N. Entropy analysis of convective MHD flow of third grade non-Newtonian fluid over a stretching sheet. Ain Shams Engineering Journal. 2017; 8(1):77-85.
3. Amanulla CH, Wakif A, Boulahia Z, Suryanarayana Reddy M, Nagendra N. Numerical investigations on magnetic field modeling for Carreau non-Newtonian fluid flow past an isothermal sphere. Journal of the Brazilian Society of Mechanical Sciences and Engineering. 2018; 40(9):462.
4. Khan M, Sardar H, Gulzar MM, Alshomrani AS. On multiple solutions of non-Newtonian Carreau fluid flow over an inclined shrinking sheet. Results in physics. 2018; 8:926-932.
5. Maleki H, Safaei MR, Alrashed AA, Kasaeian A. Flow and heat transfer in non-Newtonian nanofluids over porous surfaces. Journal of Thermal Analysis and Calorimetry. 2019; 135(3):1655-1666.
6. Mozafarie SS, Javaherdeh K. Numerical design and heat transfer analysis of a non-Newtonian fluid flow for annulus with helical fins. Engineering Science and Technology, An International Journal. 2019; 22(4):1107-1115.
7. Kempannagari AK, Buruju RR, Naramgari S, Vangala S. Effect of Joule heating on MHD non-Newtonian fluid flow past an exponentially stretching curved surface. Heat Transfer. 2020; 49(6):3575-3592.
8. Selvi R, Shukla P, Filippov AN. Flow around a liquid sphere filled with a non-Newtonian liquid and placed

into a porous medium. Colloid Journal. 2020; 82(2):152-160.
9. Ali B, Raju CS, Ali L, Hussain S, Kamran T. G-Jitter impact on magnetohydrodynamic non-Newtonian fluid over an inclined surface: Finite element simulation. Chinese Journal of Physics. 2021; 71:479-491.
10. Khashi'ie NS, Waini I, Kasim AR, Zainal NA, Ishak A, Pop I. Magnetohydrodynamic and viscous dissipation effects on radiative heat transfer of non-Newtonian fluid flow past a nonlinearly shrinking sheet: Reiner–Philippoff model. Alexandria Engineering Journal. 2022; 61(10):7605-7617.
11. Vishalakshi AB, Maranna T, Mahabaleshwar US, Laroze D. An effect of MHD on non-Newtonian fluid flow over a porous stretching/shrinking sheet with heat transfer. Applied Sciences. 2022; 12(10):4937.
12. Mahabaleshwar US, Maranna T, Perez LM, Nayakar SR. An effect of magnetohydrodynamic and radiation on axisymmetric flow of non-Newtonian fluid past a porous shrinking/stretching surface. Journal of Magnetism and Magnetic Materials. 2023; 571:170538.
13. Al Qahtani SA, Ahmad L, Khan IU, Pathak P. Local non-similar solution of radiative and magnetized flow of non-Newtonian liquid over a gravitationally affected porous surface with Newtonian heating effect. Journal of Engineering Research. 2023; 11(3):18-27.
14. Anwar MS, Irfan M, Muhammad T. Non-Newtonian fluid flow over a stretching sheet in a porous medium with variable thermal conductivity under magnetohydrodynamics influence. ZAMM-Journal of Applied Mathematics and Mechanics/Zeitschrift für Angewandte Mathematik und Mechanik. 2024; 104(12):e202301048.
15. Rekha MB, Raghunatha KR, Vinutha K, Kedia A, Chohan JS. An analytical solution of MHD non-Newtonian fluid flow over a stretching surface with mixed convection and porous media. Multiscale and Multidisciplinary Modeling, Experiments and Design. 2025; 8(1):39.
16. Kumar P, Almeida F, Nagaraja B, Ajaykumar AR. Response surface methodology for the optimisation of heat transfer rate for concatenated non-Newtonian fluid flow over a curved stretching sheet. Pramana. 2024; 99(1):10.
17. Alhazmi H, Hassan EI, Khalifa HA, Abd El-latif AM, Aldwoah K, Bilal M. Applications of thermal radiation on non-Newtonian fluid flow subject to Cattaneo-Christov heat/mass flux and double stratifications over a Riga plate. Journal of Radiation Research and Applied Sciences. 2025; 18(3):101751.
18. Almakki M, Mondal H, Mishra S. Study of viscosity variation and inconsistency of non-Newtonian fluid flow over oscillating surface. International Journal of Heat and Fluid Flow. 2026; 117:110131.
19. Abbas MS, Shaheen A, Abbas N, Shatanawi W. Dynamic analysis of radiative chemical species with non-Newtonian fluid flow over an exponentially curved stretching sheet. Proceedings of the Institution of Mechanical Engineers, Part E: Journal of Process Mechanical Engineering. 2026; 240(2):1870-1878.